Mahajan, Govinda; Thompson, Scott M.; Cho, Heejin

Article

Energy and cost savings potential of oscillating heat pipes for waste heat recovery ventilation

Energy Reports

Provided in Cooperation with:
Elsevier

Suggested Citation: Mahajan, Govinda; Thompson, Scott M.; Cho, Heejin (2017) : Energy and cost savings potential of oscillating heat pipes for waste heat recovery ventilation, Energy Reports, ISSN 2352-4847, Elsevier, Amsterdam, Vol. 3, pp. 46-53, https://doi.org/10.1016/j.egyr.2016.12.002

Energy Reports 3 (2017) 46–53

Contents lists available at ScienceDirect

Energy Reports

journal homepage: www.elsevier.com/locate/egyr

Energy and cost savings potential of oscillating heat pipes for waste heat recovery ventilation

Govinda Mahajan [a], Scott M. Thompson [b], Heejin Cho [a,*]

[a] Department of Mechanical Engineering, Mississippi State University, Mississippi State, MS 39762, United States

[b] Department of Mechanical Engineering, Auburn University, Auburn, AL 36849, United States

ARTICLE INFO

Article history:
Received 11 October 2016
Received in revised form
7 December 2016
Accepted 7 December 2016
Available online 9 March 2017

Keywords:
Oscillating heat pipe
Pulsating heat pipe
Heat recovery ventilator
Waste heat recovery

ABSTRACT

The feasibility of using finned oscillating heat pipes (OHPs) for heat exchange between counter-flowing air streams in HVAC air systems (i.e., outdoor and exhaust air flows), along with the associated cost savings in typical North American climates, is investigated. For a prescribed temperature difference and volumetric flow rate of air, rudimentary design parameters for a viable OHP Heat Recovery Ventilator (OHP-HRV) were determined using the ε-NTU (effectiveness-Number of Transfer Unit) method. The two-phase heat transfer within the OHP-HRV is modeled via effective evaporation/condensation heat transfer coefficients, while the latent heat transfer required to initiate OHP operation via boiling and evaporation is also considered. Results suggest that an OHP-HRV can possess a reasonable pressure drop ($<$200 Pa) and is capable of achieving heat recovery rate $>$5 kW. The proposed OHP-HRV can possess an effectiveness near 0.5 and can pre-cool/heat HVAC air by $>$ 5°C. Potential energy and cost savings associated with using an OHP-HRV were estimated for commercial building envelopes in various regions of the United States. It is found that the proposed OHP-HRV can save more than $2500 annually in cities that have continental climatic conditions, such as Chicago and Denver, and for the selected locations the average yearly cost savings per building is found to be on-the-order of $700. Overall, the OHP-HRV shows potential in effectively reducing energy consumption and the operational cost of air handling units in buildings.

1. Introduction

Engineering new renewable/alternate energy harvesting systems is a global priority. Discovering methods to enhance their performance while reducing their installation costs can lead to the overall reduction of end-user energy costs and greenhouse emissions. One method for accomplishing waste heat recovery in many heating, ventilation and air conditioning (HVAC) systems is to transfer heat between adjacent, enclosed air streams at different temperatures. In this way, an otherwise 'wasted' temperature potential between incoming and exhaust air streams can be beneficially utilized; as long as any air stream intrusion possesses a reasonable pressure drop. Roth et al. (2002) highlighted that air-to-air heat exchangers for the building heat recovery ventilation applications can provide a significant energy savings potential, however these devices are still not being widely adopted in US infrastructure.

Heat recovery ventilators (HRVs) are air-to-air heat exchangers that perform sensible waste heat recovery in residential, commercial, and industrial applications (Roth, 2012). They pre-condition building supply air by utilizing otherwise wasted temperature gradients between air supply and exhaust. These types of heat exchangers can be, for example, enthalpy wheels, fixed plate heat exchangers (FP-HEs), heat pipe heat exchangers (HP-HEs), and oscillating heat pipe heat recovery ventilators (OHP-HRVs). Enthalpy wheels are typically configured to rotate slowly between adjacent air streams; absorbing heat and moisture from the exhaust air and delivering it to the supply air. For equal mass flow rates in counter-flow, enthalpy wheels can achieve a sensible effectiveness on-the-order of ~80% (Shang and Besant, 2008). Pressure drops of 200–500 Pa are representative for typical flow velocities across enthalpy wheels (Casalegno et al., 2011; Markusson et al., 2010). FP-HEs are generally made of aluminum and consist of a series of plates placed equidistant to each other joined by welding, gluing, or folding. For an airflow rate of 300 CFM, FP-HEs can have a typical effectiveness of 70%–80% with pressure drops between 225–275 Pa (Roth, 2012). FP-HEs require less maintenance than enthalpy wheels as they possess no moving parts, but can require more up-front costs (Roth, 2012).

* Corresponding author.
E-mail address: cho@me.msstate.edu (H. Cho).

http://dx.doi.org/10.1016/j.egyr.2016.12.002

Nomenclature

A	Area (m^2)
A_{total}	Total heat transfer area of OHP-HRV (m^2)
A_{min}	Minimum free flow area of OHP-HRV (m^2)
A_p	Primary area of OHP (un-finned area) (m^2)
c_p	Specific heat capacity (J/kg K)
C	Total heat capacity (W/K)
C_r	Heat capacity ratio
D	Diameter (m)
D_c	Tube diameter including fin collar (m)
E_{fan}	Fan energy consumption (W)
f	Friction factor
F_p	Fin pitch (m)
G	Mass flux rate (kg/s m^2)
h	Heat transfer coefficient (kW/m^2 K)
h_{fg}	Latent heat of vaporization (J/kg)
j	Colburn j-factor
k	Thermal conductivity (W/m K)
L_1	Height of OHP-HRV (m)
L_2	Depth of OHP-HRV (m)
L_3	Width of OHP-HRV (m)
m	Fin heat transfer parameter (m^{-1})
$\dot{m}$	Mass flow rate (kg/s)
N	Number of fins
N_f	Number of fins per inch (height-wise)
N_r	Number of rows in OHP-HRV (number of OHPs)
N_t	Number of OHP-HRV tubes
NTU	Number of transfer units
Pr	Prandtl number
Q	Heat transfer rate (W)
$Q_{delivered}$	Hourly heating/cooling load (kW)
Q_{rcv}	Hourly waste heat recovery rate (kW)
R''	Thermal resistance (m^2 K/W)
r_n	Bubble radius (m)
Re	Reynolds number
S	Tube pitch (m)
T	Temperature (°C)
T_v	Vapor bubble temperature (°C)
T_{OAT}	Hourly averaged outdoor air temperature (°C)
T_{SAT}	Supply air temperature (°C)
t	Thickness (mm)
t_w	Tube wall thickness (mm)
U	Overall heat transfer coefficient (W/m^2 K)
V	Air velocity (m/s)
v	Specific volume, m^3/kg
$\dot{V}$	Volumetric air flow rate (m^3/s)
ΔE_{comp}	Hourly energy reduction while cooling (kW)
$\Delta E_{cooling}$	Hourly energy savings while cooling (kW)
$\Delta E_{furnace}$	Hourly energy reduction while heating (kW)
ΔE_{fan}	Increase in hourly fan consumption (kW)
$\Delta E_{heating}$	Hourly energy savings during winter operation (kW)
ΔE_{total}	Total hourly energy savings (kW)
ΔP	Pressure difference, kPa
ΔT	Air stream temperature difference across the OHP-HRV (°C)
$\Delta Cost_{cooling}$	Hourly cost savings while cooling ($)
$\Delta Cost_{heating}$	Hourly cost savings while heating ($)
$\Delta Cost_{el}$	Electricity cost for each location (cent/kW h)
$\Delta Cost_{ng}$	Natural gas cost for each location ($/28316.8 L) or ($/1000 cu. ft.)

Greek symbols

δ_l	Film thickness (m)
ε	OHP-HRV effectiveness
$\eta_{surface}$	Surface efficiency of outer surface of OHP tube
$\eta_{furnace}$	Furnace efficiency
μ	Dynamic viscosity (N s/m^2)
ν	Kinematic viscosity (m^2/s) or specific volume of air (m^3/kg)
ρ	Density (kg/m^3)
σ	Surface tension (N/m)
σ_f	Ratio of free-flow area to frontal area

Subscripts

1	Before heat exchanger
2	After heat exchanger
c	Condenser
c, in	*Cold air stream at inlet*
D	Diagonal
drive	Fan belt drive
f	Fin
fan	Fan
h	Evaporator
h, in	Hot air stream at inlet
i	Internal
in	Into heat exchanger
l	Liquid
L	Longitudinal
m	Mean
max	Maximum
min	Minimum
motor	Fan motor
o	Outside/overall
out	Out of heat exchanger
req	Required
S	Transverse
v	Vapor
w	Wall

HP-HEs have been investigated for their application in HVAC systems (Abd El-Baky and Mohamed, 2007; Yau and Tucker, 2003; Lamfon et al., 1998; Liu et al., 2006; Jouhara and Meskimmon, 2010). These devices are typically made of copper or aluminum (Roth, 2012) and comprise of multiple conventional-type heat pipes (CHPs) bundled together. In general, the HP-HE operating at an effectiveness of 50%–80% results in a pressure drop of 100–500 Pa for a face velocity of 400 to 800 fpm (Roth, 2012). The CHP is a two-phase heat transfer device that operates in a passive, cyclic manner (Grover and Chrisman, 1987). The device is partially filled with a pre-selected amount of working fluid (i.e. water, refrigerant, etc.) quantified via a 'fill ratio'. The prominent design of the CHP is its wicking structure (coaxial grooves, sintered particles) along its internal periphery (Peterson, 1994). During operation, liquid evaporates near the heat source (evaporator) causing vapor to flow toward the heat rejection site (condenser), where the vapor condenses and then returns to the evaporator as liquid via wicking and/or gravity. A CHP's thermal performance can be influenced by its operating orientation, and for a given design and working fluid combination, several operational limits can exist, such as the entrainment, sonic and boiling limitations (Peterson, 1994).

The oscillating heat pipe (OHP) is another type of two-phase heat transfer device; however, unlike the CHP, the OHP does not need an internal wicking structure to operate effectively. The OHP typically consists of a closed-loop, capillary structure (tube or channel) that meanders to and through a heat reception and rejection site forming multiple 'turns' (Khandekar and Groll, 2004). The OHP is partially filled with a working fluid and its internal

diameter is made sufficiently small as to ensure its capillarity, thus forming liquid slugs and vapor bubbles via surface tension. During operation, the repetitious condensation (in the condenser) and evaporation (in the evaporator) of the encapsulated working fluid creates a non-equilibrium pressure field that drives highly oscillatory fluid motion. This two-phase liquid motion results in an efficient heat transfer process consisting of both forced convection and phase change. Like the CHP, the OHP requires a minimum heat input to initiate internal fluid motion via overcoming the working fluid's latent heat of vaporization (Khandekar et al., 2003; Qu and Ma, 2007). Once this minimum, or 'start-up', heat input is acquired, the OHP can possess an effective thermal conductivity as high as 10 kW/m K (Thompson et al., 2012).

An HRV device that integrates OHP technology, i.e. an OHP-HRV, can overcome several limitations associated with other waste heat recovery devices. Unlike the enthalpy wheel, the OHP-HRV does not suffer from cross-contamination of air streams while performing heat recovery. It also possesses fewer operating limitations, and can readily attain a higher heat transfer capability relative to HP-HEs (Thompson et al., 2013; Ma, 2015). In contrast to FP-HEs that possess low manufacturability and are relatively more expensive (Andersson et al., 1987), OHP-HRVs have higher manufacturability and can hence be more cost effective.

The use of OHPs for thermal management of electronic devices has been extensively investigated for the past few decades (Miyazaki, 2005; Sarraf and Anderson, 2008; Cai et al., 2006; Maydanik et al., 2009; Katoh et al., 2004). However, the evaluation of OHPs for waste heat recovery in HVAC systems has received relatively less attention; most likely due to higher experimental setup costs. Meena et al. (2007) experimentally investigated the use of OHP-HRVs in air drying systems. The individual OHPs used were equipped with floating-ball-type check valves along portions of their capillary structure for flow control and subsequent heat transfer enhancement. Several copper-made OHPs, with an internal diameter of 2 mm, were bundled together to form the OHP-HRV, and each OHP consisted of 20 turns. The OHP-HRV used R-134a as working liquid with a filling ratio of 50%. The evaporator and condenser lengths of the OHP-HRV were each approximately 0.19 m. The OHP-HRV effectiveness was found to range between 0.29–0.76 for hot air inlet temperatures between 50 and 70 °C and flow rates between 0.5–1.0 m/s. Rittidech et al. (2005) constructed an OHP-based air preheater for a batch-type dryer for the task of waste heat recovery during a drying process. The OHP preheater consisted of 32 total OHPs each made from copper and with 8 turns. The OHP preheater was shown to be capable of achieving an effectiveness of 0.52 when R123 was used as the working fluid at a fill ratio of 50%. Supirattanakul et al. (2011) embedded a three dimensional OHP, partially filled with R-134a, into a split type air conditioning system. The embedded OHP consisted of 56 turns with evaporator, adiabatic, and condenser section lengths of 200, 190, and 200 mm, respectively. The OHP was found to result in a 14.9% improvement in the overall system coefficient of performance (COP).

The current investigation focuses on modeling and predicting the heat transfer and aerodynamic performance of a market-feasible/representative OHP-HRV, while also considering potential energy and cost savings. The evaporation and condensation heat transfer within the OHP-HRV is modeled and the effect of working fluid on OHP-HRV thermal performance is demonstrated. The energy and cost savings analysis is performed for an OHP-HRV system operating in typical HVAC environments. The potential cost benefits are demonstrated for various geographical regions within the United States, in which feasible operating climates are considered.

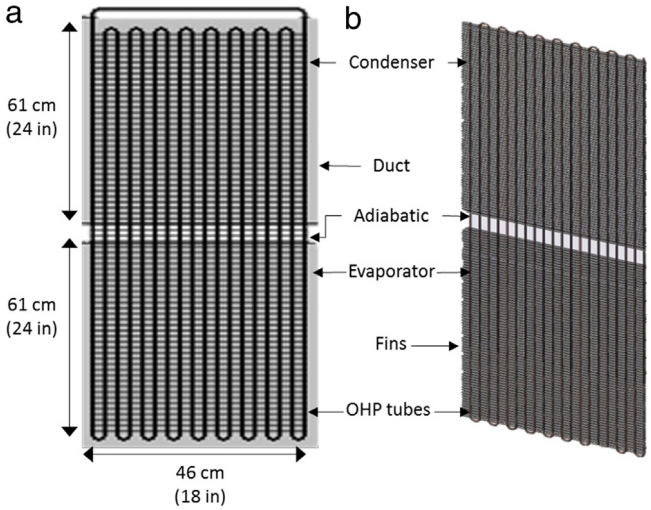

Fig. 1. (a) Front dimensioned view (a) and isometric view (b) of a unit-row OHP-HRV configured for vertically-adjacent ducts.

2. Proposed OHP-HRV design concept and operating environment

A viable design/configuration of an OHP-HRV is now described; serving as the foundation for subsequent optimization of the number of OHPs and fins used. The conceived OHP-HRV is assumed to consist of multiple, independently-operating, and finned OHPs with successive OHPs arranged in a staggered fashion (for increased heat transfer) while sharing plate fins aligned parallel to the air flow. A single-finned OHP, which is the building block of a multi-row OHP-HRV, is shown in Fig. 1; configured as to occupy the cross-sectional area, i.e. the HVAC-typical 60.96 × 45.72 cm^2, of vertically-adjacent air ducts for waste heat recovery via air-to-air heat exchange. The ducted air streams are assumed to have a uniform, volumetric flow rate ($\dot{V}$) of 1.18 m^3/s (2500 CFM) in directions opposite of each other. Outdoor (unconditioned) air temperature is assumed to vary between −8 °C (17.6 °F) and 48.9 °C (120°F).

Each OHP is assumed to be manufactured from copper capillary tubing (outer diameter = 0.318 cm, internal diameter = 0.165 cm) while consisting of pressure-fitted, 0.397 mm thick aluminum, blade-type fins. The internal diameter of the OHP tube was selected for ensuring the capillary action of acetone within the tube during standard operating conditions. Acetone was selected for its relatively low boiling temperature and viscosity. Its low toxicity and required startup heat transfer make it a reasonable choice of working fluid. As shown in Fig. 1, each OHP tube meanders through both ducts (and fins) with the closed-loop section being located outside the ducts. In practice, the relative position of the OHP-HRV evaporator to its condenser will impact its thermal performance. However, in this study, the OHP-HRV evaporator is assumed to always be positioned within the bottom duct, with its condenser in the top duct for better prediction of its heat transfer ability.

A side and top view of a multi-row OHP-HRV is provided in Fig. 2(a), where it may be seen that each row (in the axial direction) is a single OHP that shares a common blade-type fin that is perpendicular to the air flow direction. The tube-to-tube pitches (spacing) between each OHP, which are treated as constrained design variables, are shown in Fig. 2(b).

As shown in Fig. 2, two independent geometric characteristics of the OHP-HRV are the transverse pitch, S_S, and the longitudinal (axial) pitch, S_L. The diagonal pitch, S_D, is defined as:

$$S_D = \left(S_L^2 + \left(\frac{S_S}{2} \right)^2 \right)^{1/2} \quad (1)$$

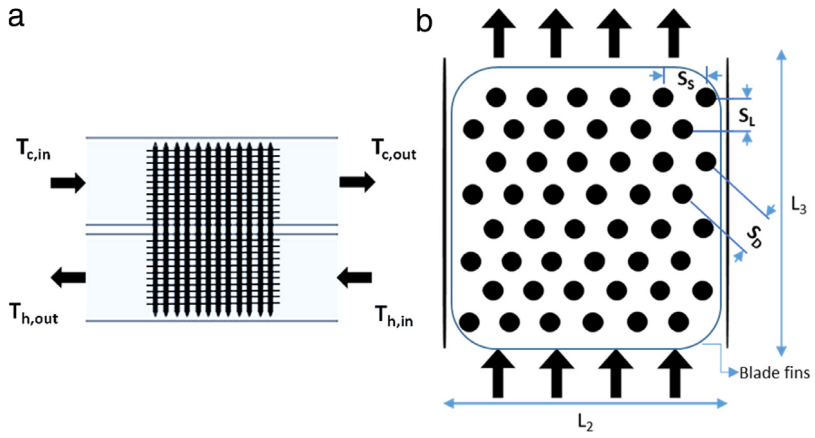

Fig. 2. OHP-HRV in adjacent ducts: (a) side view schematic and (b) top view consisting of pitch and length dimensions.

Table 1
Constrained OHP-HRV dimensions and operating conditions.

Dimension	Value	Units
OHP tube inner diameter	1.65	mm
OHP tube outer diameter	3.18	mm
OHP turn radius	1.09	cm
Number of OHP turns	20	–
Aluminum fin thickness	0.397	mm
Duct width	45.72	cm
Duct height	60.96	cm
Transverse pitch	2.18	cm
Axial pitch	1.00	cm
Evaporator-side inlet temperature	37.78	°C
Condenser-side inlet temperature	21.11	°C
Volumetric flow rate of air	1.18	m^3/s

where S_S possesses a minimum value to avoid OHP tube pinching during manufacture of its turns, and herein is set to 1.3 cm. The transverse pitch and axial pitches were held constant at 2.18 cm and 1 cm, respectively. When also considering the minimum turn radii of the OHPs, this results in each individual OHP having 20 turns. A summary of set design parameters is provided in Table 1.

3. Heat transfer and pressure drop analysis

The OHP-HRV was designed for high effectiveness while maintaining a competitive pressure drop of less than 200 Pa (US Environmental Protection Agency, 2005). The transverse and axial pitches, as well as the number of OHP turns were held constant, while the number of OHPs and the fin vertical pitch (spacing between fins) was varied. Other constrained design/operating variables are summarized in Table 1. The evaporator and condenser regions of the OHP-HRV were assumed to be two linked air-to-liquid heat exchangers (Azad and Geoola, 1984; Noie, 2006), and the heat transfer was calculated using the ε-NTU method outline in Eqs. (2)–(14). Each OHP evaporator and condenser were assigned effective heat transfer coefficients consistent with those experimentally measured and reported in the literature (Matkovic et al., 2009; Cheng et al., 2012). The heat transfer required to initiate phase-change heat transfer in the evaporator, i.e. the 'start-up' heat input was estimated by modeling the boiling heat transfer along the interior of the OHP wall. The adiabatic sections (regions with negligible heat transfer) located between the air ducts as shown in Fig. 1, were assumed to be of negligible length. The axial thermal resistance of the fluid (i.e. in duct-to-duct direction) and the vapor/liquid fraction in the evaporator (or condenser) were not considered. Further, it should be noted that the effectiveness of each OHP will depend on its location relative to the leading OHP, due to flow and thermal development effects; however, the OHP-HRV was assumed to have no temperature variation in the flow-wise or width-wise directions. All fluid properties were evaluated using a film temperature defined as the average between the surface and fluid temperatures.

The overall heat transfer coefficient, U, was found as the inverse of the sum of major thermal resistances, i.e.:

$$U = \left(R_o'' + R_w'' + R_i''\right)^{-1} \tag{2}$$

where R_o'' is the wall/air convection thermal resistance, R_w'' is the thermal resistance due to conduction along the OHP container wall, and R_i'' is the wall/fluid convection thermal resistance inside the OHP. The outer convection thermal resistance was found using:

$$R_o'' = \frac{1}{\eta_{surface} \cdot h_{air}}. \tag{3}$$

Assuming uniform, forced convection of air with uniform properties, the heat transfer coefficient for either side of the OHP-HRV, h_{air}, is given by:

$$h_{air} = j \cdot Pr^{-\frac{2}{3}} \cdot G \cdot c_p\,. \tag{4}$$

The Colburn j-factor required for Eq. (4) was found using the following relation, applicable only for $3 < N_F < 20$ (Rich, 1973):

$$j = 0.195 {Re_L}^{-0.35}. \tag{5}$$

With the Reynolds number, Re defined as:

$$Re = \frac{G \cdot S_L}{\mu}. \tag{6}$$

The tube wall thermal resistance was found using:

$$R_w'' = \frac{t_w \cdot A_o}{k_w \cdot A_i} \tag{7}$$

where the wall thickness, t_w and the thermal conductivity, k_w, were assigned values of 0.79 mm and 401 W/m K, respectively. The convection thermal resistance inside the OHP-HRV tubes was found via:

$$R_i'' = \frac{A_o}{A_i \cdot h_i} \tag{8}$$

where the internal heat transfer coefficient, h_i, was assumed to be 10 and 20 kW/m^2 K in the condenser and evaporator, respectively. These selected, order-of-magnitude values are representative of the evaporation (and/or boiling) and condensation heat transfer within an OHP (Matkovic et al., 2009; Cheng et al., 2012; Ma et al., 2008).

To estimate the heat recovery rate of the OHP-HRV, the ε-NTU method was employed, with the number of transfer units (NTU) defined as:

$$\mathrm{NTU} = \frac{U \cdot A_o}{C} \tag{9}$$

where the heat capacity rate, C, is approximately 1400 W/K for each air stream flowing at 2500 CFM in the ducting system. Acknowledging that the volumetric heat capacity of the fluid inside the OHP is much greater than the heat capacity of the passing air, due primarily to the phase-change heat transfer in the evaporator and condenser, the effectiveness for a single OHP row was approximated as (Khandekar et al., 2010):

$$\varepsilon_1 = 1 - \exp\left(-NTU\right). \tag{10}$$

The OHP-HRV, with n rows, possesses an effectiveness found via:

$$\varepsilon_n = 1 - (1 - \varepsilon_1)^n. \tag{11}$$

The effectiveness for the entire OHP-HRV using Eq. (12) as $C_c = C_h$:

$$\varepsilon = \left(\frac{1}{\varepsilon_h} + \frac{1}{\varepsilon_c}\right)^{-1} \tag{12}$$

where ε_c and ε_h are calculated for n rows using Eq. (11) and the appropriate NTU. The heat transfer through the entire OHP-HRV was then calculated using:

$$Q = \varepsilon \cdot C_{min} \cdot \left(T_{h,in} - T_{c,in}\right). \tag{13}$$

Pressure drop across OHP-HRV

The air-side pressure drop across the OHP-HRV was found using Eq. (14) (Khandekar et al., 1995):

$$\Delta P = \frac{G^2}{2} \cdot \nu_{in} \cdot \left[\left(1 + \sigma^2\right)\left(\frac{\nu_{out}}{\nu_{in}} - 1\right) + f \cdot \frac{A_{total}}{A_{min}} \cdot \frac{\nu_m}{\nu_{in}}\right] \tag{14}$$

where σ is the ratio of minimum free-flow area to frontal area and ν is the specific volume of air. The mass velocity, G is based upon the minimum free flow area of the OHP-HRV, A_{min}, which is estimated as:

$$A_{min} = \left\{\left(\frac{L_3}{S_s} - 1\right) \cdot z + \left[(S_s - D_c) - (S_s - D_o) \cdot t \cdot N_f\right]\right\} \cdot L_1 \tag{15}$$

where

$$z = \begin{cases} 2x & \text{if } 2x < 2y \\ 2y & \text{if } 2y < 2x \end{cases} \tag{16}$$

in which x and y are the dimensions of the rectangular openings between adjacent fins and tubes given by:

$$x = \frac{(S_s - D_c) - (S_L - D_c) \cdot t \cdot N_f}{2} \tag{17}$$

$$y = (S_D - D_c) - (S_L - D_c) \cdot t \cdot N_f. \tag{18}$$

The total area of the OHP-HRV, as shown by Eq. (19), is the sum of the primary area (area of un-finned tubes) and total fin area, i.e.:

$$A_{total} = A_p + A_{fin}. \tag{19}$$

The primary area and total fin area are estimated using Eqs. (20) and (21).

$$A_p = \pi \cdot D_o\left[(L_1) - t \cdot N_f \cdot L_1\right] \cdot N_t \cdot N_r \tag{20}$$

$$A_{fin} = 2\left(L_2 L_3 - \pi \frac{D_o^2}{4} N_t \cdot N_r\right) \cdot N_f \cdot L_1 + (2L_3 \cdot t \cdot N_f \cdot L_1). \tag{21}$$

The friction factor, f, is given by Eq. (22), in which Re_{Dc} is the Reynolds number based on the tube diameter including the fin collar diameter, D_c (Khandekar et al., 1995).

$$f \cong 1.039\mathrm{Re}_{D_c}^{-0.418}\left(\frac{t_f}{D_c}\right)^{-0.104} N_f^{-0.0935}\left(\frac{N_f}{D_c}\right)^{-0.197}. \tag{22}$$

4. Energy and cost savings analysis

The proposed OHP-HRV was designed for feasible integration in air-handling units (AHUs) of commercial buildings located in the US. It is assumed that the system under consideration has no recirculation of air and it is a dedicated outdoor air system (DOAS). The hourly heating/cooling energy delivered to a building area for meeting a room set-point ($Q_{delivered}$) was estimated as:

$$Q_{delivered} = \dot{V}\rho C_p\left(|T_{OAT} - T_{SAT}|\right) \tag{23}$$

where, $\dot{V}$ is the volumetric air flow rate in m^3/s, C_p is the heat capacity of the intake air, ρ is the density of air at mean temperature, T_{OAT} is the hourly averaged outdoor air temperature, and T_{SAT} is the supply air temperature for the AHU assumed to be 12 °C for summer and 40 °C for winter, which are typical setpoint temperatures in HVAC designs. The hourly waste heat recovery rate, Q_{rcv}, through the OHP-HRV was estimated as:

$$Q_{rcv} = \dot{V}\rho C_p \Delta T \tag{24}$$

where ΔT is the air stream temperature difference across the OHP-HRV condenser or evaporator region. Note that Eq. (24) was equated to Eq. (13) to obtain downstream air temperatures. Eq. (25) was used to estimate the hourly energy reduction through OHP-HRV for cooling.

$$\Delta E_{comp} = \frac{Q_{rcv}}{COP} \tag{25}$$

where COP is the coefficient of performance for a chiller assumed to be 3 in this study, which is about the minimum requirement by the ARHAE building energy standard (Khandekar, 2013). Eq. (26) was used to estimate the hourly energy reduction through OHP-HRV for heating.

$$\Delta E_{furnace} = \frac{Q_{rcv}}{\eta_{furnace}} = \frac{\dot{m} C_p \Delta T}{\eta_{furnace}} \tag{26}$$

where $\dot{m}$ is the mass flow rate of the intake air. The furnace efficiency, $\Delta E_{furnace}$ was assumed to be 0.9 for the present analysis, which is the furnace minimum requirement by the ARHAE building energy standard (Khandekar, 2013). Assuming the AHU utilizes a single-speed fan, which is commonly employed in many HVAC systems in the US commercial buildings, the pressure drop is directly proportional to the fan energy consumption and given by Eq. (27) (Khandekar, 2013):

$$\Delta E_{fan} = \frac{\dot{V} \cdot \Delta P}{\eta_{fan} \cdot \eta_{motor} \cdot \eta_{drive}} \tag{27}$$

where ΔE_{fan} is the fan energy consumption increase due to overcoming the pressure drop of the OHP-HRV, ΔP is the pressure increase in Pa determined using Eq. (14), η_{fan} is the fan energy efficiency, η_{motor} is the fan motor efficiency, and η_{drive} is the belt drive efficiency. The hourly energy savings using the proposed system for summer operation can be estimated as shown in Eq. (28).

$$\Delta E_{cooling} = \Delta E_{comp} - \Delta E_{fan}. \tag{28}$$

The hourly cost savings for cooling can be determined by Eq. (29).

$$\Delta Cost_{cooling} = \Delta E_{comp} \cdot Cost_{el} - \Delta E_{fan} \cdot Cost_{el} \tag{29}$$

Table 2
Price of natural gas and electricity for different location (US Energy Information Administration, 2013) and their climate-type (Kottek et al., 2006).

Location	Natural gas cost ($/1000 cu. ft.) (cent/kWh)	Electricity cost (cents/kWh)	Climate classification
Atlanta, GA	9.08	9.90	Humid subtropical
Baltimore, MD	10.98	10.68	Humid subtropical
Chicago, IL	11.48	8.16	Humid continental
Denver, CO	9.41	10.00	Semi-arid continental
Houston, TX	7.50	8.02	Humid subtropical
Los Angeles, CA	7.68	14.50	Mediterranean
Miami, FL	10.92	9.39	Tropical monsoon
Phoenix, AZ	10.67	9.85	Hot desert

where $Cost_{el}$ is the electricity cost for each location. The hourly energy savings using the proposed system for winter operation can be estimated as shown in Eq. (30).

$$\Delta E_{heating} = \Delta E_{furnace} - \Delta E_{fan}. \tag{30}$$

The hourly cost savings for cooling can be determined by Eq. (31).

$$\Delta Cost_{heating} = \Delta E_{furnace} \cdot Cost_{ng} - \Delta E_{fan} \cdot Cost_{el} \tag{31}$$

where $Cost_{ng}$ is the natural gas cost for each location. The total hourly energy savings using the proposed system is given by Eq. (32).

$$\Delta E_{total} = \Delta E_{cooling} + \Delta E_{heating}. \tag{32}$$

Finally, the total cost savings can be calculated by Eq. (33).

$$\Delta Cost_{total} = \Delta Cost_{cooling} + \Delta Cost_{heating}. \tag{33}$$

5. Results and discussion

After performing an optimization study, a feasible design of OHP-HRV is proposed here. The proposed OHP-HRV consists of 15 rows of 20-turns OHPs with rectangular blade-type fins at 8 mm apart and a tube-to-tube, transverse pitch of 2.18 cm. These geometric characteristics provide for a minimal pressure drop while still allowing for high heat transfer rates. For this particular OHP-HRV design, the heat transfer is 10.76 kW, corresponding to an evaporator temperature drop (pre-cooling) of 8.0 °C and a heat exchanger effectiveness of approximately 0.48. Due to air density variation, the condenser-side pressure drop is 39.8 Pa, and the evaporator-side pressure drop is 36.4 Pa. This design obtains an effectiveness within 4% of the theoretical maximum, while still achieving a low-pressure drop. These factors indicate that the proposed design may be feasible in a wide variety of applications.

An energy and cost savings analysis of the proposed OHP-HRV system described in Section 4 was performed, and the results are now presented and discussed. The proposed OHP-HRV system was designed to recover energy in an air-handling unit (AHU) that is commonly found in the US commercial building to demonstrate its energy and cost savings benefits. The AHU was assumed to be equipped with a constant speed fan of 1.18 m^3/s (2500 CFM), that has $\eta_{fan} = 0.65$, $\eta_{motor} = 0.85$, and $\eta_{drive} = 0.8$. It was also assumed that the building was under 24-h operation and that the cooling and heating was provided by a chiller and a gas furnace, respectively. The performance of the proposed OHP-HRV was evaluated in eight different US climate locations, namely: Atlanta, GA, Phoenix, AZ, Denver, CO, Los Angeles, CA, Baltimore, MD, Chicago, IL, Miami FL and Houston, TX. The outdoor air temperature data for these cities were obtained from the typical meteorological year data sets (TMY-3) (Marion and Urban, 1995) and used as inputs to determine the total energy savings by the OHP-HRV. City-wise variations in the cost of retail electricity price and natural gas for the commercial building sector were obtained from (US Energy Information Administration, 2013) (see Table 2) and used to determine cost savings using Eqs. (29), (31) and (33). Table 2 also shows the classification of the climate of cities as par as Koppen–Geiger Climate Classification System (Kottek et al., 2006).

The results of the city-wise energy and cost savings analysis is shown in Figs. 3 and 4. Fig. 3 demonstrates the season-wise potential of waste heat recovery through proposed OHP-HRV across different US cities. It may be seen that, in general, the waste heat recovery from the proposed OHP-HRV is higher for winter operation than that of summer operation. For example, sub humid tropical climatic regions, such as Atlanta and Baltimore, show that the waste heat recovery potential for winter operation accounts for more than 80% of the total annual waste heat recovery potential. Continental climatic regions, such as Chicago and Denver, show the maximum waste heat recovery potential; whereas a tropical monsoon climatic regions, such as Miami, and a Mediterranean climatic regions, such as Los Angeles, have the minimum waste heat recovery potential. This can be attributed to the fact that Chicago and Denver have approximately 8 months of winter with a monthly average temperature less than 13 °C (Marion and Urban, 1995). On the other hand, Los Angeles and Miami have approximately 8 months with average temperatures between 16 °C and 26 °C (Marion and Urban, 1995). The difference between SAT and OAT in Chicago and Denver is higher than 8 °C for most winter days. Following Fig. 3, the OHP-HRV will operate with a higher effectiveness in Chicago and Denver, where as in cities such as Los Angeles and Miami the effectiveness of OHP-HRV operation will be lower. Among the cities investigated, Phoenix – which is a region classified as hot desert – is the only city where waste heat recovery potential for summer operation is greater than that of winter operation.

Fig. 4 indicates the city-wise annual energy and cost savings potential associated with the proposed OHP-HRV. From Fig. 4, it may be seen that for an AHU of capacity 2500 CFM installed in a commercial building within these eight cities, that the average percent energy reduction is approximately 16.5%, and the average annual savings is approximately $714. Fig. 4 also demonstrates that utility rates in the respective cities play a significant role in realizing the cost savings potential of the proposed system. For example, the energy savings potential in Chicago and Denver is almost similar, but due to the difference in utility rates in these cities, Chicago has a higher cost savings potential than Denver. Likewise, Miami has a higher potential for energy savings than Los Angeles; however, Miami's cost savings potential is lower than that of Los Angeles. Baltimore and Phoenix have almost the same percentage of energy savings potential, but the cost savings potential of Baltimore is $1008 more than that of Phoenix. Atlanta and Houston have almost similar annual energy savings potential, but the annual cost savings potential of Atlanta is $614 more than that of Houston. Among these cities investigated, Houston has the cheapest utility rates and this drives its lower annual cost savings potential.

6. Conclusions

This investigation provides a first-order analysis to describe the heat transfer performance of oscillating heat pipes (OHPs) for

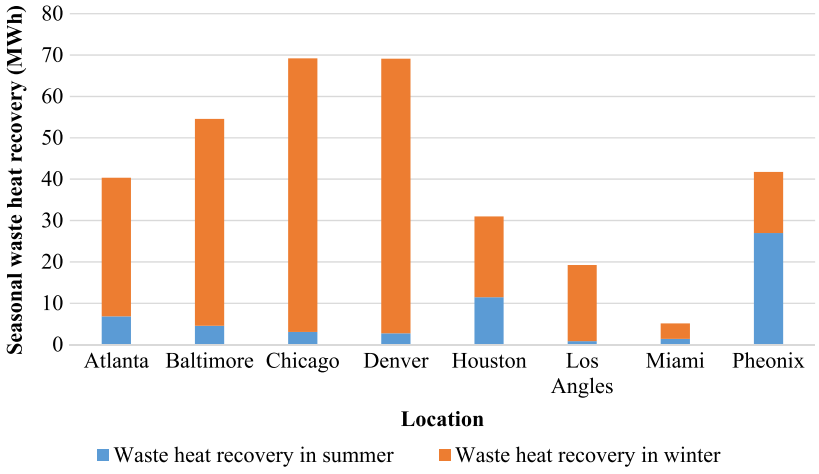

Fig. 3. Seasonal waste heat recovery through proposed OHP-HRV across different cities in the US.

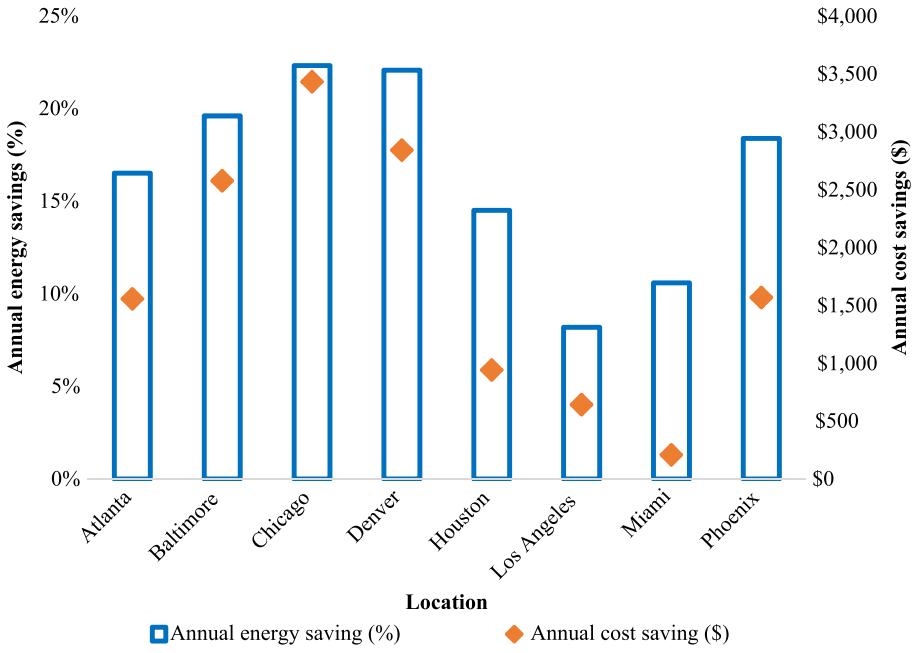

Fig. 4. Percentage annual energy and cost savings from proposed OHP-HRV for different cities in the US.

air-to-air heat exchange in a typical air conditioning system and environment. The results from the heat transfer and pressure drop analysis demonstrate that the OHP-HRV has the potential to pre-cool incoming air by 8.0 °C, with an effectiveness on the order of 0.48 and a pressure drop of approximately 40 Pa.

The results from the annual energy and cost savings analysis show that the OHP-HRV system can provide energy efficient and cost effective operation—reducing total average annual energy consumption by 16% and total annual operational cost by $714 for an AHU with an outdoor intake air flow rate of 1.18 m^3/s (2500 CFM) that provides cooling/heating for a commercial building located in eight different cities across US.

The OHP-HRV is a candidate for waste heat recovery applications since it requires no moving parts and does not require adjacent air streams to mix for optimal heat exchange. OHP-HRVs provide a cost advantage over enthalpy wheels. Although an enthalpy wheel may have a higher sensible effectiveness, the energy required for its operation, and the energy lost due to their higher pressure drop is higher. Prior to the OHP-HRV being installed for waste heat recovery, its start-up heat transfer and possible orientation-dependence must be carefully accounted for. Nonetheless, the proposed technology possesses attractive features such as: ultra-high thermal conductivity, reduced volume, reduced weight and an aerodynamic design with low pressure drop. These features have the potential to result in lower manufacturing cost, lower set-up costs and reduced operational cost for ventilation, heating and cooling systems.

Acknowledgments

The work presented herein was financially supported by Mississippi State University's Bagley College of Engineering and Department of Mechanical Engineering. Authors would also like to thank contributions made by Charles McCullough.

References

Abd El-Baky, M.A., Mohamed, M.M., 2007. Heat pipe heat exchanger for heat recovery in air conditioning. Appl. Therm. Eng. 27, 795–801.
Andersson, J., Edso, L., Jonsson, N.A., Rissler, P., 1987. Plate heat exchanger.
2012. ASHRAE, ASHRAE Handbook- HVAC Systems and Equipment, Atlanta, GA.
2013. ASHRAE. ASHRAE Handbook- Fundamentals, Atlanta, GA, p. 404.

2013. ASHARE, Standard 90.1-2013. Energy Standard for Buildings Except Low-Rise Residential Buildings, Atlanta, GA.
Azad, E., Geoola, F., 1984. A design procedure for gravity-assisted heat pipe heat exchanger. J. Heat Recovery Syst. 4 (2), 101–111.
Cai, Q., Chen, C.-L., Asfia, J.F., 2006. Heat transfer enhancement of planar pulsating heat pipe device. In: Heat Transfer, Vol. 2. ASME, pp. 153–158.
Casalegno, A., De Antonellis, S., Colombo, L., Rinaldi, F., 2011. Design of an innovative enthalpy wheel based humidification system for polymer electrolyte fuel cell. Int. J. Hydrog. Energy 36 (8), 5000–5009.
Cheng, P., Dong, J., Thompson, S.M., Ma, H.B., 2012. Heat transfer in the bulk and thin film fluid regions of a rectangular micro groove. J. Thermophys. Heat Transfer 26 (1), 108–114.
Grover, G.M., Chrisman, R.H., 1987. Heat pipe.
Jouhara, H., Meskimmon, R., 2010. Experimental investigation of wraparound loop heat pipe heat exchanger used in energy efficient air handling units. Energy 35 (12), 4592–4599.
Katoh, T., Vogel, M., Xu, G., Novotny, S., 2004. Heatlane technology for high heat flux chip cooling. In: Heat Transfer, Vol. 1. ASME, pp. 69–74.
Kays, W.M., London, A.L., 1955. Compact Heat Exchangers: A Summary of Basic Heat Transfer and Flow Friction Design Data. National Press.
Khandekar, S., 2010. Pulsating heat pipe based heat exchangers. In: Proc. 21st Int. Symp. Transp. Phenom., (iii), pp. 2–5.
Khandekar, S., Dollinger, N., Groll, M., 2003. Understanding operational regimes of closed loop pulsating heat pipes: an experimental study. Appl. Therm. Eng. 23 (6), 707–719.
Khandekar, S., Groll, M., 2004. An insight into thermo-hydrodynamic coupling in closed loop pulsating heat pipes. Int. J. Therm. Sci. 43, 13–20.
Kottek, M., Grieser, J., Beck, C., Rudolf, B., Rubel, F., 2006. World map of the Köppen-Geiger climate classification updated. Meteorol. Z. 15 (3), 259–263.
Lamfon, N.J., Najjar, Y.S.H., Akyurt, M., 1998. Modeling and simulation of combined gas turbine engine and heat pipe system for waste heat recovery and utilization. Energy Convers. Manage. 39 (1), 81–86.
Liu, D., Tang, G.-F., Zhao, F.-Y., Wang, H.-Q., 2006. Modeling and experimental investigation of looped separate heat pipe as waste heat recovery facility. Appl. Therm. Eng. 26 (17), 2433–2441.
Ma, H., 2015. Oscillating heat pipes. In: Oscillating Heat Pipes. Springer-Verlag, New York.
Ma, H.B., Borgmeyer, B., Cheng, P., Zhang, Y., 2008. Heat transport capability in an oscillating heat pipe. J. Heat Transfer 130 (8), 081501.
Marion, W., Urban, K., 1995. User's Manual for TMY2s. National Renewable Energy Laboratory, Golden, Colorado, USA.
Markusson, C., Jagemar, L., Fahlén, P., 2010. Energy recovery in air handling systems in non-residential buildings-design considerations. In: ASHRAE Transactions 2010 Annual Conference Albuquerque, NM, JUN 26-30, 2010, pp. 154–167.
Matkovic, M., Cavallini, A., Del Col, D., Rossetto, L., 2009. Experimental study on condensation heat transfer inside a single circular minichannel. Int. J. Heat Mass Transfer 52 (9–10), 2311–2323.
Maydanik, Y.F., Dmitrin, V.I., Pastukhov, V.G., 2009. Compact cooler for electronics on the basis of a pulsating heat pipe. Appl. Therm. Eng. 29 (17–18), 3511–3517.
Meena, P., Rittidech, S., Poomsa-ad, N., 2007. Application of closed-loop oscillating heat-pipe with check valves (CLOHP/CV) air-preheater for reduced relative-humidity in drying systems. Appl. Energy 84 (5), 553–564.
Miyazaki, Y., 2005. Cooling of notebook pcs by flexible oscillating heat pipes. In: Advances in Electronic Packaging, Parts A, B, and C. ASME, pp. 65–69.
Noie, S.H., 2006. Investigation of thermal performance of an air-to-air thermosyphon heat exchanger using ε-NTU method. Appl. Therm. Eng. 26 (5–6), 559–567.
Peterson, G.P., 1994. An Introduction to Heat Pipes. Modeling, Testing, and Applications. Wiley, New York, Chichester.
Qu, W., Ma, H.B., 2007. Theoretical analysis of startup of a pulsating heat pipe. Int. J. Heat Mass Transfer 50, 2309–2316.
Rich, D.G., 1973. The effect of fin spacing on the heat transfer and friction performance of multi-row, plate fin-and-tube heat exchangers. AsHRAE Trans. 79 (2), 137–145.
Rittidech, S., Dangeton, W., Soponronnarit, S., 2005. Closed-ended oscillating heat-pipe (CEOHP) air-preheater for energy thrift in a dryer. Appl. Energy 81, 198–208.
Roth, K.W., Westphalan, D., Dieckmann, J., Hamilton, S.D., Goetzler, W., 2002. Energy consumption characteristics of commercial building HVAC systems volume III: Energy savings potential. In: TIAX LLC, Cambridge, MA, 2002.
Sarraf, D.B., Anderson, W.G., 2008. High temperature and high heat flux thermal management for electronics, In: International Conference and Exhibition on High Temperature Electronics 2008, HiTEC 2008, pp. 33–39.
Shang, W., Besant, R.W., 2008. Theoretical and experimental methods for the sensible effectiveness of air-to-air energy recovery wheels. HVAC&R Res. 14 (3), 373–396.
Supirattanakul, P., Rittidech, S., Bubphachot, B., 2011. Application of a closed-loop oscillating heat pipe with check valves (CLOHP/CV) on performance enhancement in air conditioning system. Energy Build. 43 (7), 1531–1535.
Thompson, S.M., Tessler, B.S., Ma, H.B., Smith, D.E., Sobel, A., 2012. Ultra-high thermal conductivity of three-dimensional flat-plate oscillating heat pipes for electromagnetic launcher cooling. In: Proceedings of IEEE 2012 16th International Symposium on Electromagnetic Launch Technology, EML, Beiging, China.
Thompson, S.M., Tessler, B.S., Ma, H., Smith, D.E., Sobel, A., 2013. Ultrahigh thermal conductivity of three-dimensional flat-plate sscillating heat pipes for electromagnetic launcher cooling. IEEE Trans. Plasma Sci. 41 (5), 1326–1331.
US Energy Information Administration, 2013. Electric Power Annual 2012. US Department of Energy, Washington, DC, USA.
US Environmental Protection Agency, 2005. Low Pressure - Drop HVAC Design for Laboratories, DOE/GO-102005-2042. US Department of Energy, Washington, DC, USA.
Yau, Y.H., Tucker, A.S., 2003. The performance study of a wet six-row heat-pipe heat exchanger operating in tropical buildings. Int. J. Energy Res. 27 (3), 187–202.